

Synthesis and photovoltaic effect of vertically aligned ZnO/ZnS core/shell nanowire arrays

K. Wang,¹ J. J. Chen,¹ Z. M. Zeng,¹ J. Tarr,¹ W. L. Zhou,^{1,a)} Y. Zhang,^{2,b)} Y. F. Yan,³ C. S. Jiang,³ J. Pern,³ and A. Mascarenhas³

¹Advanced Materials Research Institute, University of New Orleans, New Orleans, Louisiana 70148, USA

²Department of Electrical and Computer Engineering, University of North Carolina at Charlotte, Charlotte, North Carolina 28223, USA

³National Renewable Energy Laboratory, Golden, Colorado 80401, USA

(Received 15 January 2010; accepted 25 February 2010; published online 23 March 2010)

A vertically aligned ZnO/ZnS core/shell nanowire array with type II band alignment was directly synthesized on an indium-tin-oxide glass substrate and the photovoltaic effect of the nanowire array was investigated. The epitaxial relationship, wurtzite (0001) matching zinc-blende (111), was observed in the ZnO/ZnS nano-heterostructure. ZnS coating is found to quench the photoluminescence of ZnO nanowires but enhance the photocurrent with faster response in the photovoltaic device, indicating improvement in charge separation and collection in the type II core/shell nanowire. © 2010 American Institute of Physics. [doi:10.1063/1.3367706]

The use of quasi-one-dimensional, vertically aligned nanostructures to construct three-dimensional architectures as building blocks for photovoltaic (PV) devices, boosting charge transport and collection and/or enhancing light absorption, has demonstrated advantages over conventional planar devices.^{1–4} To facilitate efficient charge separation, great efforts have been made to adopt the lateral *p-n* junctions for the device geometry based on the core/shell nanowires.^{3,5–8} Recently, an alternative strategy relying on type II band alignment has been proposed to achieve the lateral charge separation in the core/shell nanowire solar cells.^{9,10} This approach uses the “quasielectric force” of the heterostructure,¹¹ in contrast to the real electric field of the *p-n* junction, and it should remain functional even when the size is reduced to the quantum region.¹² For mesoscopic scale devices,^{3,5} combining two operational mechanisms, *p-n* junction and type II junction, will allow a greater flexibility in optimizing the cell performance. In the true nano scale, the band gap tunability of the type II junction could extend the selection of active layer materials to the wide-band gap semiconductors.^{9,10} Furthermore, ZnO and ZnS core/shell structure are expected to be useful for photo-detector applications.

Efficient charge separation facilitated by type II heterojunction has been reported in several nanocrystal systems.^{13,14} In our previous work, we also demonstrated the synthesis of a highly lattice-mismatched ZnO/ZnSe core/shell nanowire array with type II band alignment for exploring the potential of building all-inorganic stable nanostructured solar cells.¹⁵ However, there are few reports of nanowire based devices realizing the proposed core/shell type II heterojunction concept. In this paper, we report the synthesis of a vertically aligned ZnO/ZnS nanowire array on indium tin oxide (ITO)-coated glass substrates and the observation of the photovoltaic effect based on the nanostructured nanowire array.

The ZnO/ZnS core/shell nanowire array was fabricated by a two-step synthesis, and the detailed procedures were similar to our previous work.¹⁵ Briefly, vertically aligned ZnO nanowire arrays were first synthesized by chemical vapor deposition (CVD) on an ITO substrate at 600 °C. The nanowire array then served as a template for further ZnS coating by pulsed-laser deposition (PLD) at 500 °C. The devices were fabricated using a technique of fabricating three-dimensional nanodevices based on vertically aligned nanowire arrays.¹⁶

Figure 1(a) shows a typical scanning electron microscope (SEM) image of an as-synthesized ZnO nanowire array, revealing perpendicular growth of ZnO nanowires on the ITO glass with an average length of $\sim 7 \mu\text{m}$ and diameters in the range of 50–120 nm. SEM image of the nanowire array after the PLD of ZnS is presented in Fig. 1(b). Compared to the bare ZnO nanowire, we found a noticeable increase in the diameter and rough surface for the ZnO/ZnS nanowires, which implies that ZnS is deposited over the ZnO nanowire. X-ray diffraction (XRD) patterns of the bare and

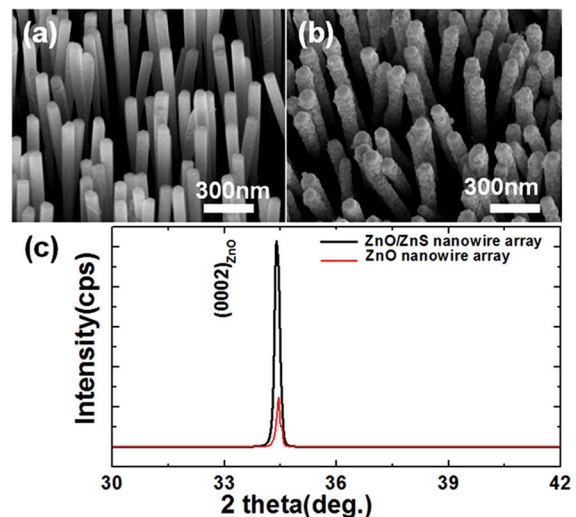


FIG. 1. (Color online) [(a) and (b)] SEM images of bare ZnO and ZnO/ZnS core/shell nanowire arrays, respectively. (c) XRD patterns of ZnO and ZnO/ZnS nanowire arrays.

^{a)} Author to whom correspondence should be addressed. Electronic mail: wzhou@uno.edu.

^{b)} Electronic mail: yong.zhang@uncc.edu.

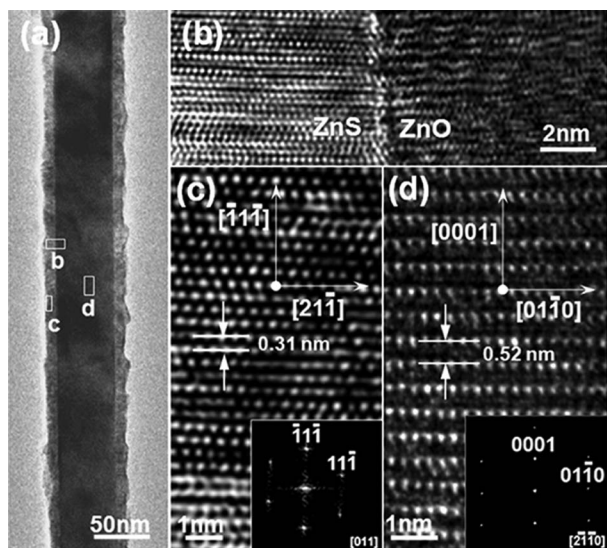


FIG. 2. Structural characterization of ZnO/ZnS core/shell nanowire array. (a) Low-magnification TEM micrograph of a ZnO/ZnS core/shell nanowire. (b) High-resolution TEM image of the interface of the core/shell heterostructure, enlarged from the rectangular area in (a), showing the epitaxial growth relationship of ZnO wurtzite core and ZnS zinc-blende shell. [(c) and (d)] Atomic resolution images of the core and shell areas taken from the rectangular areas in (a), respectively. The insets in (c) and (d) represent the corresponding FFT patterns.

shelled ZnO nanowire array are shown in Fig. 1(c). Only the strong hexagonal ZnO (0002) diffraction peak was observed in XRD patterns for the bare ZnO nanowire array, indicating strong preferred orientation along the *c* axis of wurtzite (WZ) ZnO. For the XRD pattern of the ZnO/ZnS nanowire array, the intensity of the (0002) peak from ZnO increased significantly because the PLD was performed at the relatively high temperature of 500 °C; thus, the crystalline quality of the ZnO core was improved as a result of an annealing effect. No additional diffraction peak was observed in the pattern of ZnO/ZnS nanowires, perhaps because the ZnS layer is fairly thin. However, a slight position shift of the ZnO peak to a lower angle was observed for the ZnO/ZnS core/shell structure, which indicates the presence of lattice expansion caused by the strain.

Figure 2(a) shows a typical low-magnification transmission electron microscope (TEM) image of a ZnO/ZnS core/shell nanowire. The sharp interface between the core and shell clearly shows that the ZnO nanowire is fully sheathed by a ZnS layer along the entire length. The ZnS layer is ~12 nm thick and has a rough surface. Figure 2(b) is a high-resolution TEM image of the rectangular area b in Fig. 2(a) that shows the detailed interface structure between the ZnO core and ZnS shell. Although lattice distortion (in ZnO) and stacking faults (in ZnS) can be observed along the interface, both the core and shell exhibit lattice fringes and can be further identified as WZ and zinc-blende (ZB) structures, respectively, thus indicating that the ZnS shell layer was grown over the ZnO core. To achieve more precise information about the growth relationship, the magnified TEM image of the core and shell taken from rectangles c and d in Fig. 2(a) and their corresponding fast Fourier transform (FFT) patterns are shown in Figs. 2(c) and 2(d). The marked interplanar *d* spacings of 0.31 and 0.52 nm correspond, respectively, to the ($\bar{1}\bar{1}\bar{1}$) lattice plane of ZB ZnS with the [011] zone axis and the (0001) lattice plane of WZ ZnO with the $[2\bar{1}\bar{1}0]$ zone

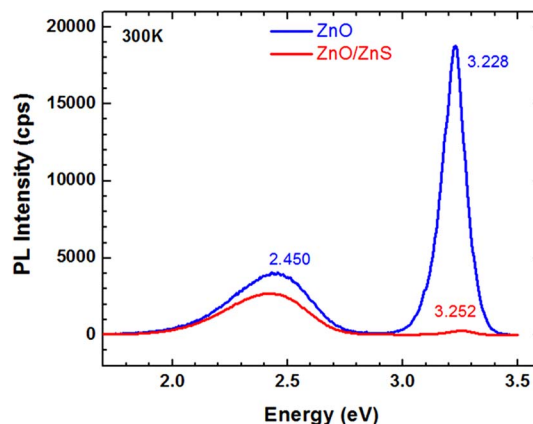


FIG. 3. (Color online) Room-temperature photoluminescence spectra of ZnO and ZnO/ZnS core/shell nanowire arrays.

axis. Thus, the core and shell are determined as epitaxial growth with the growth relationship of $[0001]_{\text{ZnO}} \parallel [\bar{1}\bar{1}\bar{1}]_{\text{ZnS}}$ and $[01\bar{1}0]_{\text{ZnO}} \parallel [21\bar{1}]_{\text{ZnS}}$, in contrast to that for the previously studied ZnO/ZnSe system, where $[0001]_{\text{ZnO}} \parallel [001]_{\text{ZnSe}}$ was observed.¹⁵

The optical properties of the ZnO/ZnS core/shell nanowire were investigated by photoluminescence (PL) spectroscopy. Figure 3 shows the PL spectra of ZnO and ZnO/ZnS nanowire arrays measured at room temperature. The PL spectrum of the bare ZnO nanowire array consists of two emission peaks at 3.228 and 2.450 eV. Although close to the band gap, the higher energy peak is still likely defect- or impurity-related, because for high-quality bulk ZnO, the room-temperature emission peak has been found at somewhat higher energy, for instance, 3.265 eV.¹⁵ The lower energy peak is obviously non-intrinsic and is often believed to be associated with oxygen-vacancy¹⁷ or surface-related states,¹⁸ although the exact origin of this transition remains unclear. Compared with the bare ZnO nanowire array, the peak position of the UV emission in ZnO/ZnS sample shows a small blue shift, and the intensity is reduced by a factor of 63. The intensity of the visible peak is also reduced, but to a much lesser extent (by ~30%). Qualitatively, the effect of a ZnS coating is similar to that of a ZnSe coating reported previously.¹⁵ It was recently reported that a ZnS coating over ZnO nanotubes or nanorods enhanced UV emission,^{19,20} which appears to agree with conventional wisdom that (1) the coating of a large-band gap material diminishes the loss through surface recombination and (2) the UV emission is from the bulk part of the ZnO. However, this understanding is not expected to hold true for type II combinations such as ZnO/ZnS, even though ZnS has a larger band gap. In principle, one should expect that the charge-separation effect quenches, instead of enhances, the PL signal, because the type II core/shell structure should result in depleting the holes in the ZnO core. However, if this mechanism were indeed responsible for the observed quenching of the UV emission in our core/shell structure, we should have seen the quenching of both UV and visible emission to a similar degree. This result should also hold true if the coating introduces nonradiative defect centers at the heterojunction interface. That the reduction is relatively small for the visible peak and much more significant for the UV peak may suggest that the visible emission could be from the bulk part of the ZnO nanowire, whereas the UV emission could be sur-

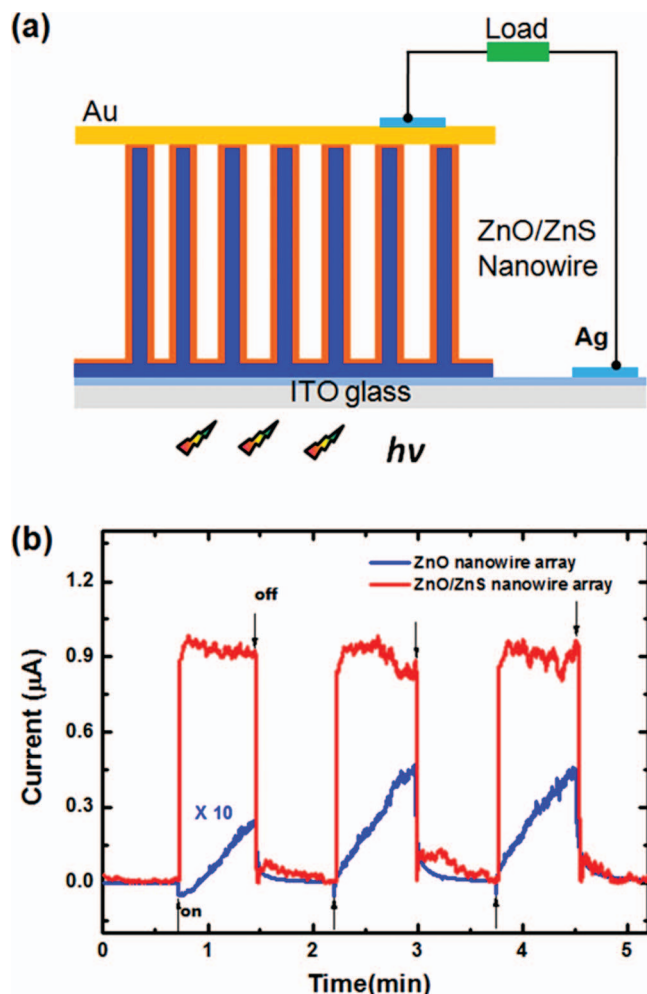


FIG. 4. (Color) (a) Schematic structure of the PV device based on a type II core/shell nanowire array utilized for photoresponse measurement; (b) Time-dependent photocurrent of bare ZnO and ZnO/ZnS core/shell nanowire arrays without external bias.

face related and thus more sensitive to the coating that has modified the electronic structure of the bare ZnO nanowire surface, either by introducing nonradiative centers or inducing the transfer of holes to the ZnS shell from the surface bound excitons.

We fabricated a prototype PV device, as shown schematically in Fig. 4(a), using the ZnO/ZnS core/shell nanowire array as the active layer and carrier transport medium, and ITO and gold as the anode and cathode, respectively. The time-dependent photocurrent was measured without external bias, as shown in Fig. 4(b). The photocurrent responded (rose/decayed) instantly as the incident light was turned on/off. Although the photocurrent increase was also observed in the device composed of a bare ZnO nanowire array, the signal was about 30 times weaker for the same device size that was roughly determined by the contacted area. Moreover, the photoresponse observed in the ZnO device was slower than that in the ZnO/ZnS device, which may be attributed mainly to a heating effect or surface-related adsorbates (O_2^-).²¹ The enhanced photocurrent and faster response observed in ZnO/ZnS, together with the quenching of the UV emission, could indicate the realization of the key feature of the type II heterostructure-charge separation, although we cannot exclude other possibilities (such as the ZnS/Au contact is different from ZnO/Au). However, be-

cause of the large thickness of the nanowire layer, light absorption occurs mostly in the bulk part of the ZnO nanowire core, the core/shell interface has to serve the function of separating the electrons and holes.

In conclusion, we demonstrated the epitaxial growth of a highly mismatched semiconductor nanoheterostructure, ZnO/ZnS, in the geometry of a core/shell nanowire. The structural study revealed the epitaxial relationship of the heterostructure of two crystalline phases, ZnO-(0001)/ZnS-(111), adding to our recent report of ZnO-(0001)/ZnSe-(001), which shows very intriguing growth phenomena important for the future study in nano-heterostructure growth. The charge separation in the ZnO/ZnS core/shell nanowire array was investigated by PL spectroscopy and photoresponse. The type II heterojunction-based device could expand the opportunities for designing and optimizing nanoscale PV and other optoelectronic devices beyond the conventional *p-n* junction approach.

The work performed at UNO was supported by the DARPA under Grant No. HR0011-07-1-0032, research grants from Louisiana Board of Regents under Contract No. LEQSF (2008–11)-RD-B-10 and LEQSF (2007–12)-ENH-PKSFI-PRS-04, and American Chemical Society Petroleum Research Fund under PRF No 48796-DN110. The work at UNC-Charlotte was partially supported by CRI. The authors acknowledge Professor M. Tarr for polishing the manuscript for English.

- ¹M. Law, L. E. Greene, J. C. Johnson, R. Saykally, and P. Yang, *Nature Mater.* **4**, 455 (2005).
- ²Z. Y. Fan, H. Razavi, J. W. Do, A. Moriwaki, O. Ergen, Y. L. Chueh, P. W. Leu, J. C. Ho, T. Takahashi, L. A. Reichertz, S. Neale, K. Yu, M. Wu, J. W. Ager, and A. Javey, *Nature Mater.* **8**, 648 (2009).
- ³B. M. Kayes, H. A. Atwater, and N. S. Lewis, *J. Appl. Phys.* **97**, 114302 (2005).
- ⁴Y. B. Tang, Z. H. Chen, H. S. Song, C. S. Lee, H. T. Cong, H. M. Cheng, W. J. Zhang, I. Bello, and S. T. Lee, *Nano Lett.* **8**, 4191 (2008).
- ⁵B. Tian, X. Zheng, T. J. Kempa, Y. Fang, N. Yu, G. Yu, J. Huang, and C. M. Lieber, *Nature (London)* **449**, 885 (2007).
- ⁶J. A. Czaban, D. A. Thompson, and R. R. LaPierre, *Nano Lett.* **9**, 148 (2009).
- ⁷E. C. Garnett and P. Yang, *J. Am. Chem. Soc.* **130**, 9224 (2008).
- ⁸H. Goto, K. Nosaki, K. Tomioka, S. Hara, K. Hiruma, J. Motohisa, and T. Fukui, *Appl. Phys. Express* **2**, 035004 (2009).
- ⁹Y. Zhang, L. W. Wang, and A. Mascarenhas, *Nano Lett.* **7**, 1264 (2007).
- ¹⁰J. Schrier, D. O. Demchenko, L. W. Wang, and A. P. Alivisatos, *Nano Lett.* **7**, 2377 (2007).
- ¹¹H. Kroemer, in *Nobel Lectures in Physics (1996–2000)*, edited by G. Ekspong (World Scientific, Singapore, 2002).
- ¹²Y. Zhang, in *SPIE Newroom*, edited by J. Pern, A. Mascarenhas, and W. Zhou (SPIE, Bellingham, WA, 2008).
- ¹³B. O. Dabbousi, J. RodriguezViejo, F. V. Mikulec, J. R. Heine, H. Mattoussi, R. Ober, K. F. Jensen, and M. G. Bawendi, *J. Phys. Chem. B* **101**, 9463 (1997).
- ¹⁴R. S. Zeng, T. T. Zhang, J. C. Liu, S. Hu, Q. Wan, X. M. Liu, Z. W. Peng, and B. S. Zou, *Nanotechnology* **20**, 095102 (2009).
- ¹⁵K. Wang, J. J. Chen, W. L. Zhou, Y. Zhang, Y. F. Yan, J. Pern, and A. Mascarenhas, *Adv. Mater.* **20**, 3248 (2008).
- ¹⁶B. B. Cao, J. J. Chen, X. J. Tang, and W. L. Zhou, *J. Mater. Chem.* **19**, 2323 (2009).
- ¹⁷V. A. Fonoberov, K. A. Alim, A. A. Balandin, F. X. Xiu, and J. L. Liu, *Phys. Rev. B* **73**, 165317 (2006).
- ¹⁸B. D. Yao, Y. F. Chan, and N. Wang, *Appl. Phys. Lett.* **81**, 757 (2002).
- ¹⁹H. C. Liao, P. C. Kuo, C. C. Lin, and S. Y. Chen, *J. Vac. Sci. Technol. B* **24**, 2198 (2006).
- ²⁰Y. M. Yu, M. H. Hyun, S. Nam, D. Lee, B. O. K. S. Lee, P. Y. Yu, and Y. D. Choi, *J. Appl. Phys.* **91**, 9429 (2002).
- ²¹C. Soci, A. Zhang, B. Xiang, S. A. Dayeh, D. P. R. Aplin, J. Park, X. Y. Bao, Y. H. Lo, and D. Wang, *Nano Lett.* **7**, 1003 (2007).